The Structure and Evolution of Convection in a Tropical Cloud Cluster[1]

COLLEEN A. LEARY[2] AND ROBERT A. HOUZE, JR.

Department of Atmospheric Sciences, University of Washington, Seattle 98195

(Manuscript received 13 June 1978, in final form 6 October 1978)

ABSTRACT

A large cloud cluster which occurred over the data network of the Global Atmospheric Research Program's Atlantic Tropical Experiment (GATE) on 5 September 1974 is examined. Data from four quantitative shipboard weather radars show that virtually all of the precipitation in the tropical cloud cluster was associated with six mesoscale precipitation features. A prototype for the structure and life cycle of these features is presented which is sufficiently general to describe all six precipitation features, one of which was a tropical squall-line system. These mesoscale features appear to be the primary entities within which deep tropical convection occurs.

In their formative stage, mesoscale precipitation features consist of a line of isolated cumulonimbus cells oriented perpendicular to the low-level wind flow.

In the intensifying stage, the rain areas of the individual cells merge when new convective cells develop between and ahead of the existing cells, where the outflow from convective-scale downdrafts enhances low-level convergence. In the upper troposphere an overhang of cloud and precipitation particles extends downwind in the layer of outflow from deep convective updrafts.

The mature mesoscale precipitation feature possesses both a region of convective cells along its leading edge and a large area of horizontally uniform precipitation to the rear. The longevity and total rainfall in the area of horizontally uniform precipitation suggest that its maintenance may be due to organized mesoscale uplift in an anvil cloud extending from the 600–700 mb level to the upper troposphere. In the horizontally uniform rain area beneath the anvil cloud, aircraft observations show cold, dry, low-θ_w air consistent with the presence of a mesoscale unsaturated downdraft maintained by cooling due to the evaporation of falling rain. A pronounced radar bright band at the melting level is further evidence of cooling in this region.

In the dissipating stage, intense convective cells cease forming along the leading edge but the area of horizontally uniform precipitation persists for at least several hours longer.

Interactions among the six mesoscale precipitation features result in echo mergers that complicate the precipitation pattern of the cloud cluster, and give the cloud cluster of 5 September a distinctive double shape.

1. Introduction

Much of the deep convection over the tropical oceans occurs in cloud clusters (Martin and Karst, 1969; Martin and Suomi, 1972; Frank, 1970; GARP Report, 1970) which consist of many individual cumulonimbus towers whose high-level outflow forms a common cirrus shield. The importance of the convection in cloud clusters to the atmospheric general circulation was anticipated by Riehl and Malkus (1958) who showed that a balanced tropical heat budget requires vertical transports of mass and heat which can only be accomplished in nearly undilute cumulonimbus towers extending from the top of the boundary layer to the upper troposphere. Gray (1968), Yanai *et al.* (1973), Ogura and Cho (1973) and Johnson (1976) have explained heat and moisture budgets of the large-scale environment in the vicinity of cloud clusters in terms of compensating downward motion between convective towers and the detrainment of water from the tops of convective updrafts. Yanai *et al.* (1973), however, recognized that their method of computing the bulk properties of a population of convective clouds was a simplified one and that more accurate formulations, including the effects of mesoscale organization of cumulus convection and a more realistic parameterization of precipitation processes, require a knowledge of the internal structure of cloud clusters.

That some cloud clusters possess a distinctive structure including mesoscale organization has been established by Zipser (1969, 1977), Betts (1976) and Houze (1977). They have studied tropical squall-line systems of the type which Payne and McGarry (1977) distinguish from other cloud clusters on satellite photographs by a more rapid propagation speed, an oval-shaped cirrus shield, and an arc-shaped leading edge.

[1] Contribution No. 477, Department of Atmospheric Sciences, University of Washington.

[2] Current affiliation: Atmospheric Science Group, Texas Tech University, Lubbock 79409.

0022-4928/79/030437-21$09.25

These squall-line systems possess, in addition to deep cumulonimbus towers along the leading edge, a mesoscale downdraft beneath a precipitating anvil cloud to the rear of the active cumulonimbus towers. Such a mesoscale downdraft as well as a mesoscale updraft in the anvil cloud have been simulated by Brown (1979) in a numerical model.

This paper examines the structure and evolution of convection in the double cloud cluster in the trough of the easterly wave that passed over the data network of the Global Atmospheric Research Program's Atlantic Tropical Experiment (GATE) on 5 September 1974. The relationship between the convection in this cloud cluster and the wind field on scales of and larger than the cloud cluster has been described by Leary (1979). In this paper, we extend the model of the tropical squall-line system proposed by Houze (1977) to describe the structure of convection in a cloud cluster that possesses none of the distinguishing features of a squall-line cloud cluster. In so doing, we arrive at a more general concept, that of the mseoscale precipitation feature, of which the tropical squall-line system is a particularly well-developed example.

2. Data

The GATE radar data was the principal source of information about the structure and evolution of convection in the 5 September cloud cluster for this study. Fig. 4 illustrates the positions of the four ships carrying quantitative radars and indicates their overlapping coverage. Houze (1977) has described the GATE radar data, and his Table 1 lists the characteristics of the four C-band radars.

In conjunction with the radar data, we used other GATE data to define further and interpret physically the behavior of convection in the cloud cluster.

Leary (1979) has described the analysis of the GATE surface and rawinsonde data to obtain the wind field in the vicinity of the 5 September cloud cluster throughout its lifetime.

Visible and infrared satellite imagery from the geosynchronous SMS-1 satellite, obtained from the *GATE Data Catalog* (EDS, 1975) and the Space Science and Engineering Center at the University of Wisconsin were used to define the upper level cirrus shield of the cloud cluster, to identify active convection beyond the range of the GATE radars, and to identify and follow distinctive nonprecipitating features in the cloudiness pattern.

Aircraft data processed by the National Center for Atmospheric Research (NCAR) and obtainable through the *GATE Data Catalog* (EDS, 1975) include four flights that penetrated the cloud cluster of 5 September. Data from the United Kingdom C-130 at 150 m, the NCAR Electra L-188 at 450 m, the National Oceanic and Atmospheric Administration (NOAA) DC-6 at 1500 m, and the National Aeronautics and Space Administration (NASA) CV-990 at 11.9 km were used to study variations in wind flow and thermodynamic properties inside the cloud cluster.

3. A prototype for the three-dimensional structure and life cycle of the mesoscale features that made up the precipitation pattern of the cloud cluster

The precipitation pattern observed with the four GATE radars on 5 September was a complex one. Individual echoes covered areas ranging in size from a few to more than 10^4 km^2 and moved in different directions with varying speeds. Within this wealth of detail, six mesoscale features in the precipitation pattern stood out. One of these was the squall-line system whose structure and dynamics have been described by Houze (1977). The squall-line system was itself an independent cloud cluster which formed early on 4 September. During 5 September it merged with the other mesoscale features making up the cloud cluster which we examine in this paper.

The six mesoscale precipitation features comprising the 5 September cloud cluster possessed structures and life cycles of striking similarity, leading us to the generalization that there exists a characteristic mesoscale organization of precipitation in tropical cloud clusters. Fig. 1 presents this organization in schematic form as viewed by radar in both horizontal and vertical cross sections of the four stages in the life cycle of an individual mesoscale feature. The prototype shown in Fig. 1 is an extension of the model of a mature squall-line system proposed by Houze (1977). In this extended model the entire life cycle of a mesoscale precipitation feature, as well as the structure and behavior of a wider variety of mesoscale precipitation features are included.

a. Formative stage

In its formative stage (Fig. 1a), the mesoscale precipitation feature consists of a line of isolated radar echoes. In vertical cross section, the echoes have the vertically oriented reflectivity contours associated with convective precipitation. Although small in horizontal dimension and considerably shallower than more intense, deeper convection, these showers commonly contain rainfall rates of 10 mm h^{-1} or more. At this stage, the radar-observed echo structure shown in Fig. 1a is typical, not only of situations that later develop into mesoscale precipitation areas of great intensity, but also of lines of weak echoes that dissipate without further development. The factor that controls development is, therefore, not structural but dynamical. Those bands of echoes that dissipate without developing into mesoscale precipitation features are aligned parallel to and move in the same direction as the winds near the surface. Bands of isolated echoes that later develop into more intense features are aligned more

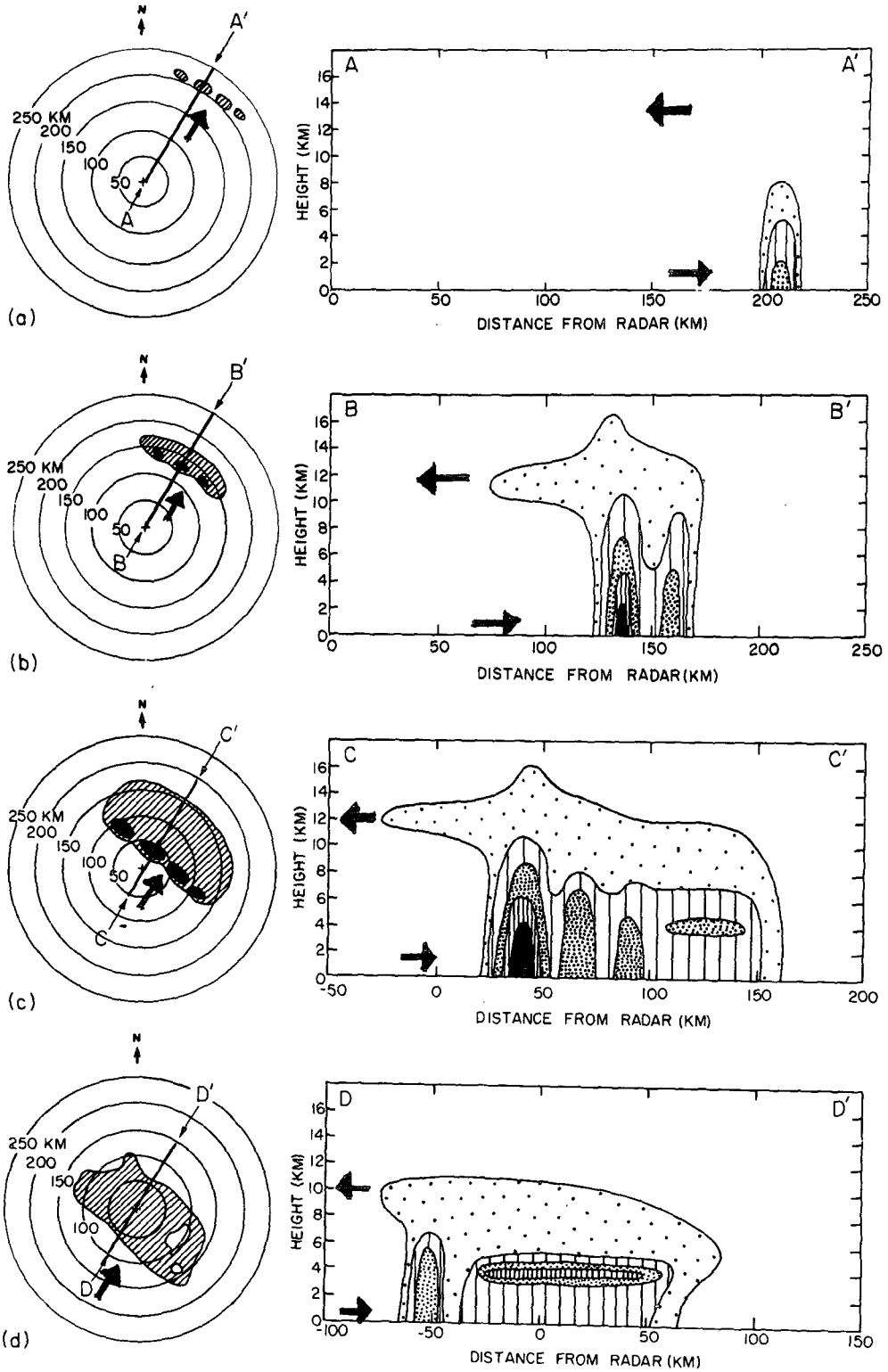

FIG. 1. Schematic of the structure of a mesoscale precipitation feature as viewed by radar in horizontal and vertical cross sections during the (a) formative, (b) intensifying, (c) mature and (d) dissipating stages of its life cycle. The outside contour of radar reflectivity is the weakest detectable echo, and the inner contours are for successively higher reflectivity values. Heavy arrows on horizontal cross sections indicate direction of the low-level winds. Arrows on vertical cross sections indicate directions of the low-level and upper-level winds.

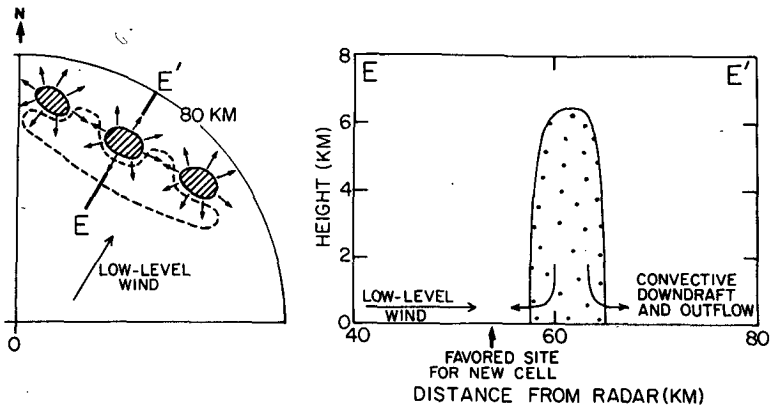

FIG. 2. Schematic showing the development of new convective cells between and ahead of existing cells (area outlined by dashed line) due to enhanced low-level convergence in the vicinity of convective downdrafts.

nearly perpendicular to the low-level winds and move in a direction opposite to these winds.

The low-level outflow from convective-scale downdrafts in shallow echoes aligned perpendicular to the low-level winds can modify the local pattern of low-level convergence so as to favor the formation of new convective cells along and on the upwind (with respect to the low-level winds) side of the band. If we assume that outflow from convective-scale downdrafts associated with shallow echoes is radially outward, low-level convergence is enhanced at the sites between the individual echoes making up the band and also upwind of each individual echo. The enhanced convergence makes these sites favorable locations for new convective cells to form. Fig. 2 illustrates this process schematically.

b. Intensifying stage

Development in the upwind direction contributes to the propagation speed of the mesoscale feature and marks the transition to the intensifying stage of its life cycle (Fig. 1b). New cells form along the leading (forward) edge before the older ones to the rear can dissipate. This leads to a broadening of the intensifying mesoscale feature to a width of two or more convective cells. As new convective cells develop between older ones along the band, the echoes associated with them merge with the older ones to form a single, larger, elongated echo in which the newer cells appear as intense convective cores. At the same time, the height of the echoes increases to the level of the tropopause. These cells are the hot towers whose existence was inferred by Riehl and Malkus (1958). Surface precipitation rates associated with these deep embedded convective cells can exceed 100 mm h^{-1}. Upper level winds carry cloud and precipitation particles downwind from the tops of the cells to form the cirrus shield that is so prominent in satellite photographs of cloud clusters and an overhang of precipitation particles aloft. Fig. 1b shows such an overhang spreading in advance of the surface precipitation pattern. This configuration is not the only possible one. Upper level winds directing blowoff toward the rear of or parallel to the echo at the surface are also observed.

c. Mature stage

In several respects, the mature stage in the life cycle of a mesoscale precipitation feature (Fig. 1c) resembles the intensifying stage. The mature feature exhibits extensive echo development both in the surface precipitation pattern and in vertical cross section. Deep, intense convective cells along the leading edge are accompanied by the heaviest rain at the surface. Precipitation particles generated in the more intense updrafts continue to overshoot the tropopause, and the upper level winds carry precipitation and cloud particles downwind of the cell tops.

The major structural difference between the intensifying stage and the mature stage is the development of an extensive region of horizontally uniform precipitation to the rear of the intense convective cells in the mature precipitation feature. This region was formerly occupied by intense convective cells which blended together as they dissipated at the rear of the propagating zone of intense convection developing along the leading edge of the feature. As the cells dissipate they become weaker, diffuse and ultimately indistinguishable from each other in the trailing portion of the mesoscale feature. As described in detail and illustrated schematically by Leary and Houze (1979), this horizontally uniform region is characterized by a bright band of high radar reflectivity in the melting layer, just below the 0°C isotherm. A horizontally stratified reflectivity pattern covering such an extensive area is inconsistent with the presence of convective-scale updrafts and downdrafts there. Thermodynamic observations suggest that a mesoscale downdraft, initiated and sustained by melting and evaporation of falling precipitation, exists in

this region. Surface rainfall rates on the order of 3 mm h^{-1} are typical in the area of horizontally uniform precipitation.

d. Dissipating stage

The transition between the mature stage (Fig. 1c) and the dissipating stage (Fig. 1d) is a gradual one. The intense convective cells which continue to form along the leading edge are increasingly shallow and have less intense rainfall at the surface as time progresses, and eventually cease forming altogether. The large region of horizontally uniform precipitation then slowly dissipates until only a few scattered fragments of the large uniform echo mass remain. The cessation of active convection suggests that either the convergence in the large-scale low-level wind flow which supplies warm moist air to convective updrafts or some other aspect of dynamic forcing becomes deficient, or that thermodynamic changes in the environment of the mesoscale precipitation features—possibly those produced by the extensive deep convection itself—eventually inhibit further intense convection.

Unlike the first three stages, which each typically last for between 1 and 5 h, the dissipating stage may last for 8 h or more. This relatively long interval is due to the persistence of the area of horizontally uniform precipitation after new development ceases. Its large area and long lifetime make the region of horizontally uniform precipitation an important contributor to the total rainfall associated with the mesoscale precipitation feature. As suggested by Houze (1977) and by the numerical experiments of Brown (1979), the maintenance of this horizontally uniform precipitation over such a large area for so long a time may be aided by widespread lifting in a thick, anvil cloud whose base is at about the 600–700 mb level and whose top lies in the upper troposphere near the level of outflow from cumulonimbus updrafts.

4. Identification of mesoscale precipitation features

The low-level precipitation pattern observed by the four GATE radars during the lifetime of the cloud cluster is shown in Fig. 3. The size and longevity (see Table 1) of the six features labeled N, SQ, W1, W2, E1 and E2 clearly place them in the category of mesoscale features. Since virtually all of the precipitation which fell in the cloud cluster was associated with these six mesoscale features, a description of their evolution constitutes a description of the life cycle of the precipitation pattern of the cloud cluster as a whole. As an aid to the discussion of the rather complex precipitation pattern shown in Fig. 3, Fig. 4 depicts the mesoscale features in schematic form, including, where appropriate, their velocities during 6 h periods on 5 September. No velocity vectors are shown in Fig. 4 for precipitation features that remain motionless, lose their identities, or move in or out of radar range during a 6 h period.

TABLE 1. Size and longevity of the mesoscale features that made up the precipitation pattern of the 5 September 1974 cloud cluster.

Mesoscale feature	Lifetime (h)	Maximum horizontal dimension (km)
SQ	>23	360
N	8	580
E1	24	220
E2	14	190
W1	12	340
W2	>16	460

At the beginning of the day, a long band of isolated echoes (N in Fig. 4a) to the north was moving southward between 0000 and 0600 GMT[3]. In the observed radar precipitation pattern, N was centered at 10.5°N, 23°W at 0000 (Fig. 3a) and at 9.5°N, 24°W at 0600 (Fig. 3b). Southeast of feature N lay a band of echoes oriented from northwest to southeast (E1 in Fig. 4a). Feature E1 was located at 9°N, 20.5°W at 0000 (Fig. 3a), and moved southwestward to 8.5°N, 21°W at 0600 (Fig. 3b). To the southwest of feature E1 lay the precipitation areas remaining from the squall-line system (SQ) studied by Houze (1977). These, labeled SQA and SQB in Fig. 4a, behaved in two different ways. The largest echo SQA centered at 7.5°N, 24.5°W at 0000 (Fig. 3a), continued to move westward. At 0600 it was located at 7.5°N, 25°W (Fig. 3). A smaller but still distinct group of echoes (SQB) associated with the northeastern portion of the squall-line system moved in a northeasterly direction. At 0000 these were centered at 8.5°N, 23.5°W (Fig. 3a) and by 0600 had reached 9°N, 23°W (Fig. 3b). To the northwest of SQA and SQB, a band of echoes oriented from northwest to southeast (W1 in Fig. 4a) moved southeastward, until at 0600 it was located at 8.5°N, 24.5°W (Fig. 3b).

The period between 0600 and 1200 was a time of great change in the character of the precipitation pattern, during which it acquired a distinctive double structure. As feature N moved southward it evolved into two mesoscale features, W2 and E2 in Fig. 4b. W2 moved rapidly southwestward to overtake feature W1, which remained nearly motionless between 0600 and 1200. The merger of features W1 and W2 produced the western half of the double cloud cluster (Leary, 1979, Fig. 1), which was centered at 9°N, 25°W at 1200 (Fig. 3d). By this time, E2 had expanded, giving E1 and E2 the appearance of a single large precipitation area. This temporary merger of E1 and E2, centered at 9°N, 22°W, formed the eastern half of the double cloud cluster. Between 0600 and 1200 feature SQA

[3] All times are GMT.

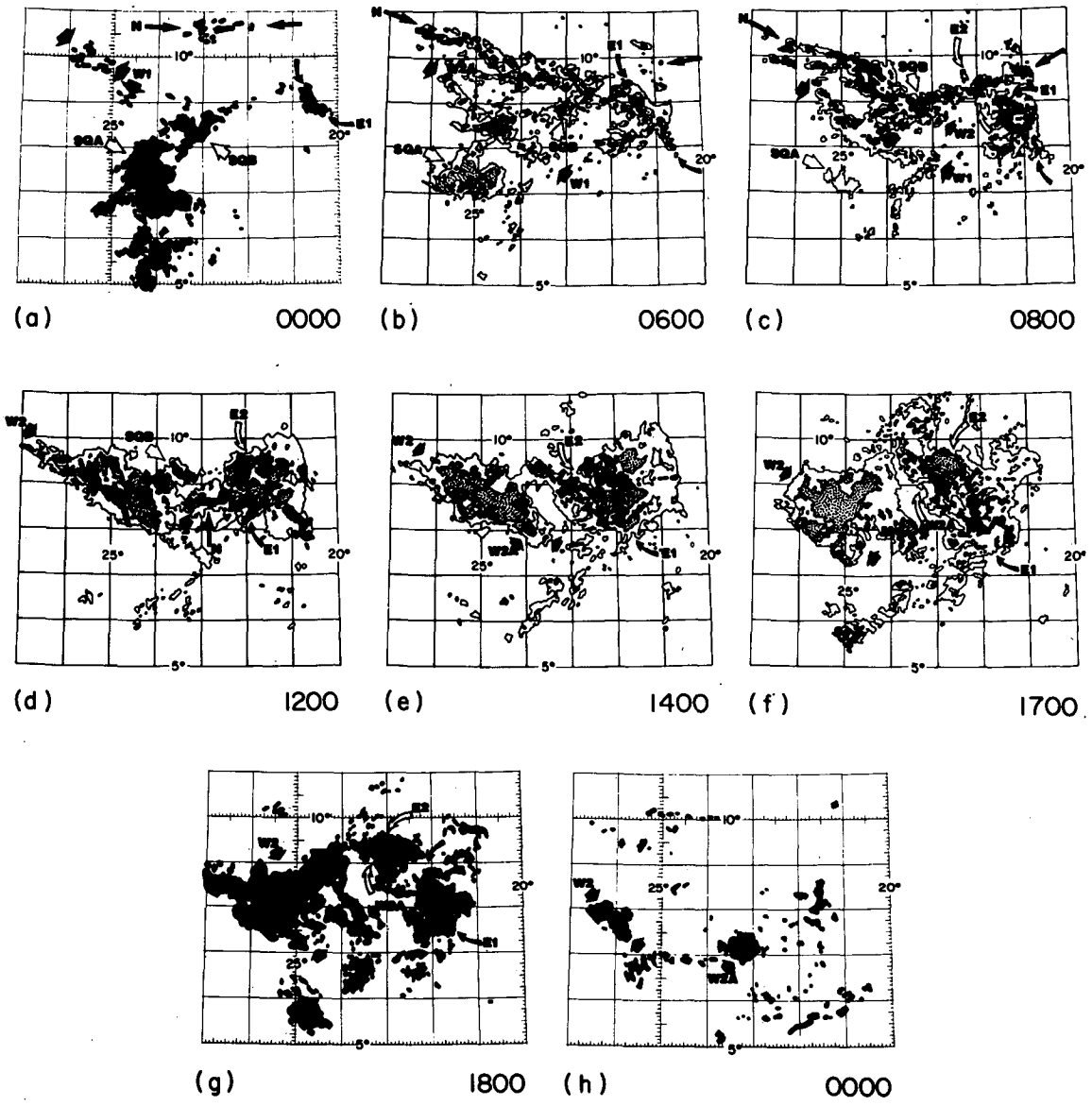

FIG. 3. Evolution of the precipitation pattern associated with the cloud cluster of 5 September 1974 as seen in composites of data from the four GATE radars. On (b), (c), (d), (e) and (f) the outside contour is for the weakest detectable echo and the inside contours are for 32 dBZ or 5 mm h^{-1} and 40 dBZ or 20 mm h^{-1}. On (a), (g) and (h) the area occupied by echoes is shaded black.

moved westward out of radar range (Fig. 4b). The only other remnant of the squall-line system, SQB, merged with N (Fig. 3c) and the developing feature W2.

During the 6 h interval between 1200 and 1800, depicted schematically in Fig. 4c, no major precipitation areas formed, and intense convection throughout the cloud cluster was on the decline. South of features W2 and E1, a series of lines of small echoes, oriented from northeast to southwest, moved northeastward without achieving great intensity. In the western half of the cloud cluster, W2 continued to move southwestward (Fig. 4c), until at 1800 it was centered at 8.5°N, 25.5°W (Fig. 3g). A portion of the southeastern corner of W2, labeled W2A in Fig. 4c, began to move southeastward during the interval, even though it remained loosely connected to the larger precipitation area. In the eastern half of the cloud cluster, features E1 and E2 regained their separate identities (Figs. 3f, 4c) as they moved apart and precipitation in the area joining them ceased.

Between 1800 on 5 September and 0000 on 6 September (Fig. 4d), the rain areas of the cloud cluster largely dissipated. Of all the mesoscale features, only W2 retained its identity until the end of the day. At 0000 on 6 September (Fig. 3h) it was located at 7.5°N, 26°W. At that time it was passing out of the range of the GATE radars. Feature W2A broke away from W2 during this period and continued moving southeastward.

It merged with an isolated echo (Fig. 4d) that was moving northeastward. The isolated echo was a remnant of the line of echoes shown moving northeastward in Fig. 4c. Features E1 and E2 completely dissipated between 1800 and 0000. At 0000 on 6 September (Fig. 4h), with the exception of W2 and W2A, only small isolated echoes not associated with any major precipitation area remained in the area formerly occupied by intense convection.

5. The life cycles, three-dimensional structures and interactions of the mesoscale precipitation features

The six mesoscale precipitation features identified in Section 4 passed through life histories from which the prototype discussed in Section 3 was deduced, and they interacted with one another to produce the precipitation pattern of the double cloud cluster. Fig. 5 summarizes schematically the interactions between individual bands that influenced their development. The following subsections describe the life cycles and structures of the observed mesoscale features, and how interactions with each other and with isolated smaller echoes influenced their development. The squall-line system (SQ) has been described in detail by Houze (1977). In this section we confine the discussion of SQ to its interactions with the other mesoscale precipitation features, and its similarity to them in structure and behavior.

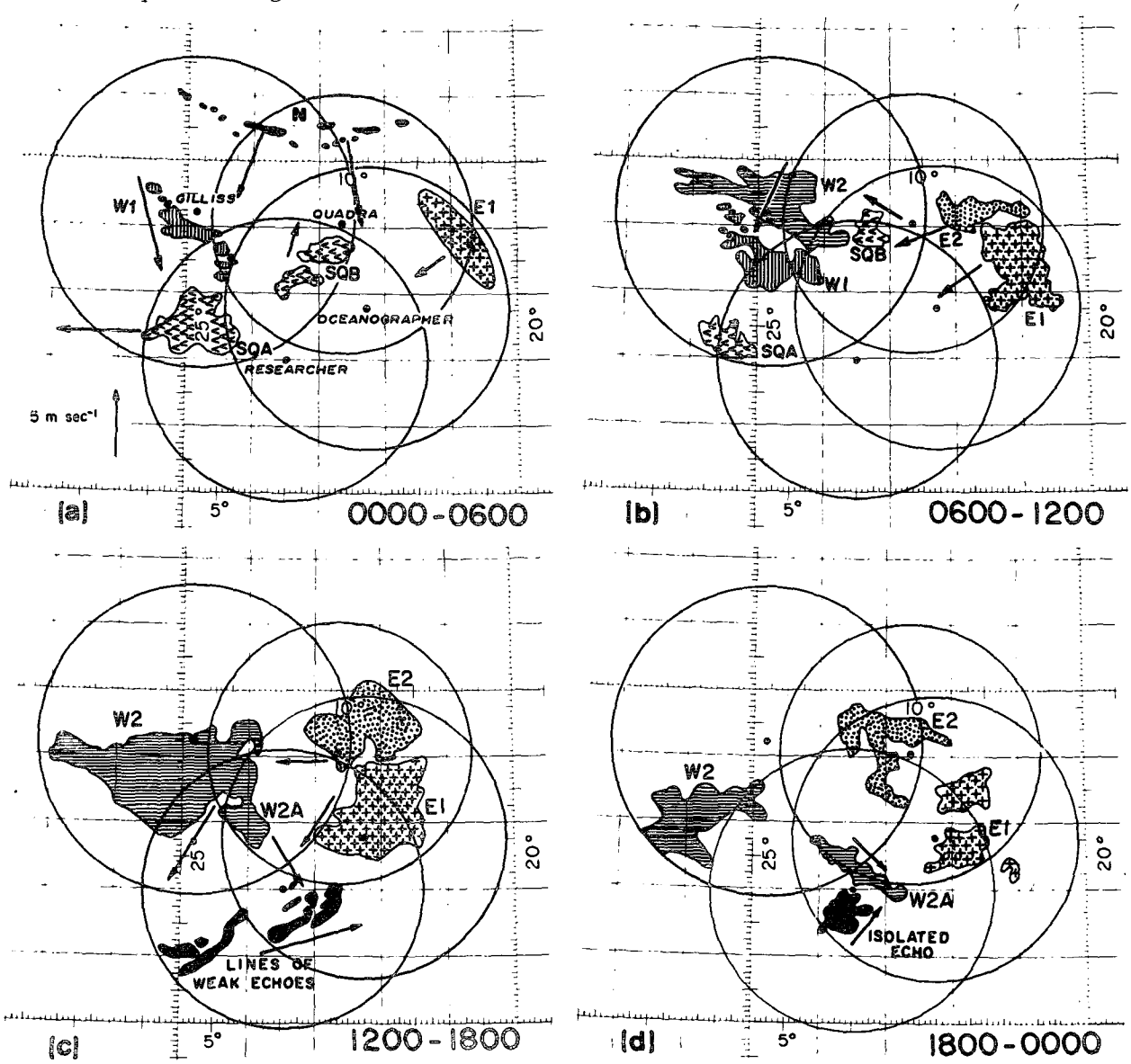

FIG. 4. Schematic of the evolution and movement of the mesoscale precipitation features in the cloud cluster of 5 September 1974. The four circles outline the range of the four GATE radars. Symbols denote the mesoscale precipitation features discussed in the text. Times are GMT.

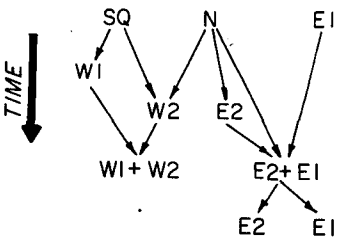

FIG. 5. Schematic showing the interactions (denoted by arrows) among the mesoscale precipitation features (identified by symbols) which make up the precipitation pattern of the cloud cluster of 5 September 1974.

a. Feature E1

Feature E1 was already in the intensifying stage when it first appeared on the periphery of the *Oceanographer* radar scope early in the day on 5 September (Fig. 6a). Its component convective elements had merged to form a single band. The surface winds were southwesterly and westerly (Fig. 2a of Leary, 1979) in the vicinity of E1, which was moving toward the southwest. Thus, the surface winds blew perpendicular to E1 and opposite to its direction of motion. This enhanced the low-level convergence at the leading edge of E1, to favor further development. Between 0900 and 1145 (Figs. 6c–6d), E1 acquired an extensive area of light rain to the rear of its leading edge as it matured.

Fig. 7 shows E1 as viewed in horizontal and vertical cross sections during the intensifying (Fig. 7a), maturing (Fig. 7b) and dissipating (Fig. 7c) stages of its life cycle. Most of the features of the prototype (Fig. 1) appear in Fig. 7. An overhang of precipitation particles aloft developed and extended ahead of the surface precipitation pattern. This feature can be seen in all of the vertical cross sections shown in Fig. 7. The direction in which the overhang emanated from the lower level echo was downwind of the 200 mb flow relative to

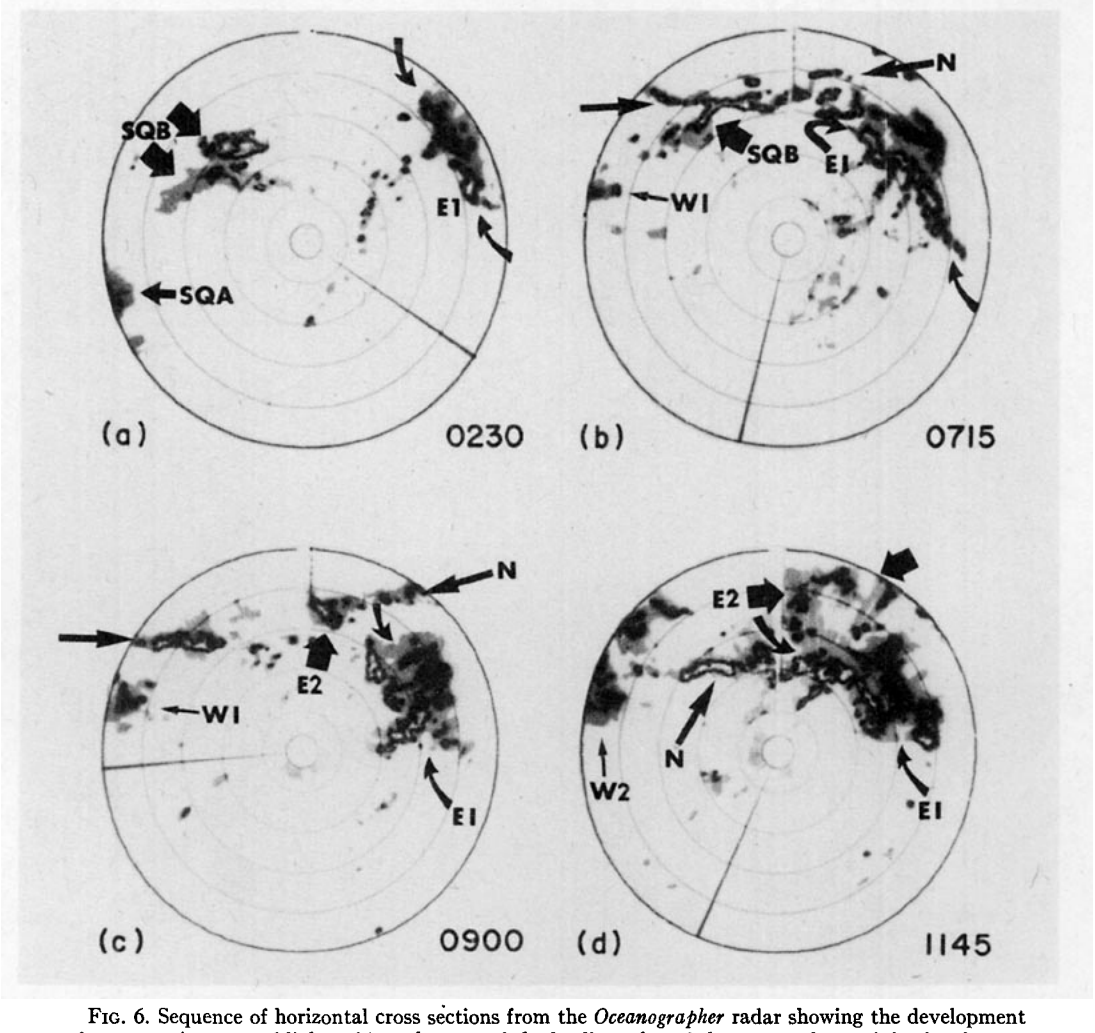

FIG. 6. Sequence of horizontal cross sections from the *Oceanographer* radar showing the development of an extensive area of light rain to the rear of the leading edge of the mesoscale precipitation feature E1 on 5 September 1974. Shading thresholds are for weakest detectable echo (gray), 31 dBZ or 4 mm h^{-1} (black), 39 dBZ or 17 mm h^{-1} (white), 47 dBZ or 74 mm h^{-1} (gray). Range marks are at 18.5, 46.5, 93, 139.5, 186 and 232.5 km. Times are GMT.

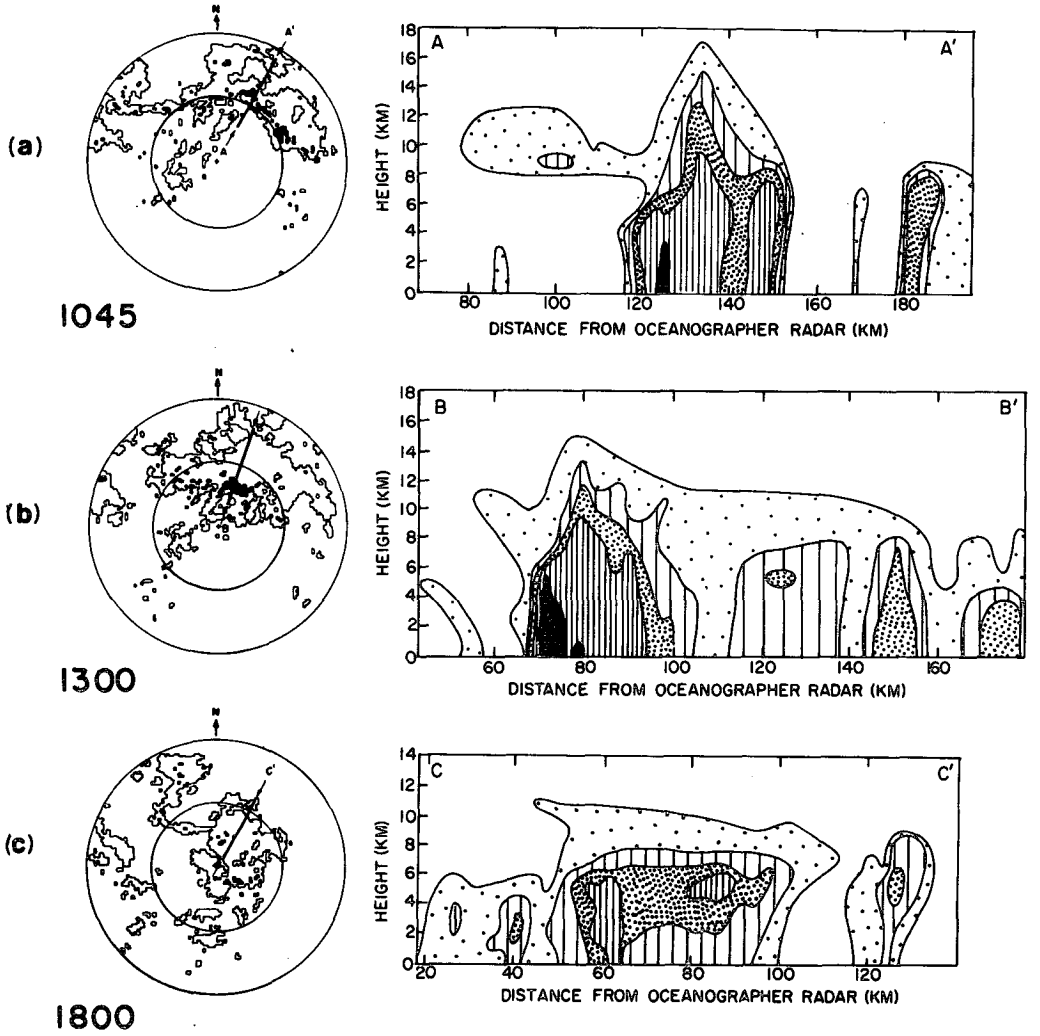

FIG. 7. Mesoscale precipitation feature E1 as viewed by the *Oceanographer* radar in horizontal and vertical cross sections during the (a) intensifying, (b) mature and (c) dissipating stages of its life cycle. Outside contour on horizontal cross sections is for the minimum detectable echo, inner contour is for 38 dBZ or 14 mm h^{-1}, range marks are at 110 and 220 km, and labeled lines identify the vertical cross sections. Outside contour on vertical cross sections is for the weakest detectable echo, and inner contours are for 23, 28, 33 and 43 dBZ. Times are GMT on 5 September 1974.

E1 (Leary, 1979, Fig. 2). The area of horizontally uniform precipitation during the dissipating stage of E1 was located at a range too great for the vertical resolution inherent in the scanning procedure followed by the GATE radars to establish the presence or absence of a bright band at the melting level. However, the horizontal homogeneity of the echo pattern in Fig. 7c suggests that had it been closer to the ship, the radar would have detected a bright band. The area of horizontally uniform precipitation persisted for more than 6 h (Figs. 3e–3g) after the area of intense convective cells had begun to shrink in size.

Feature E1 was unique among the mesoscale features of the double cloud cluster because research aircraft traverses through it provided wind and thermodynamic observations of high resolution along the flight tracks. Fig. 8 presents a synthesis of aircraft and radar data which suggests that a mesoscale downdraft existed in the region of horizontally uniform precipitation. Both temperature and dewpoint (Fig. 8b) at the 450 m level were lower in the area of the horizontally uniform precipitation (the intervals between 1215 and 1222, and from 1227–1228) than in the region where warm, moist air ahead of the advancing line of convection was flowing toward the area of active convection (e.g., the interval between 1232 and 1235). The wet-bulb potential temperature θ_w showed a variation of 2° between the region of horizontally uniform precipitation and the region of low-level convergent inflow. Since θ_w is conserved in moist adiabatic processes, and because θ_w decreases upward in the tropical atmosphere to about the 4 km level, we infer the presence of a meso-

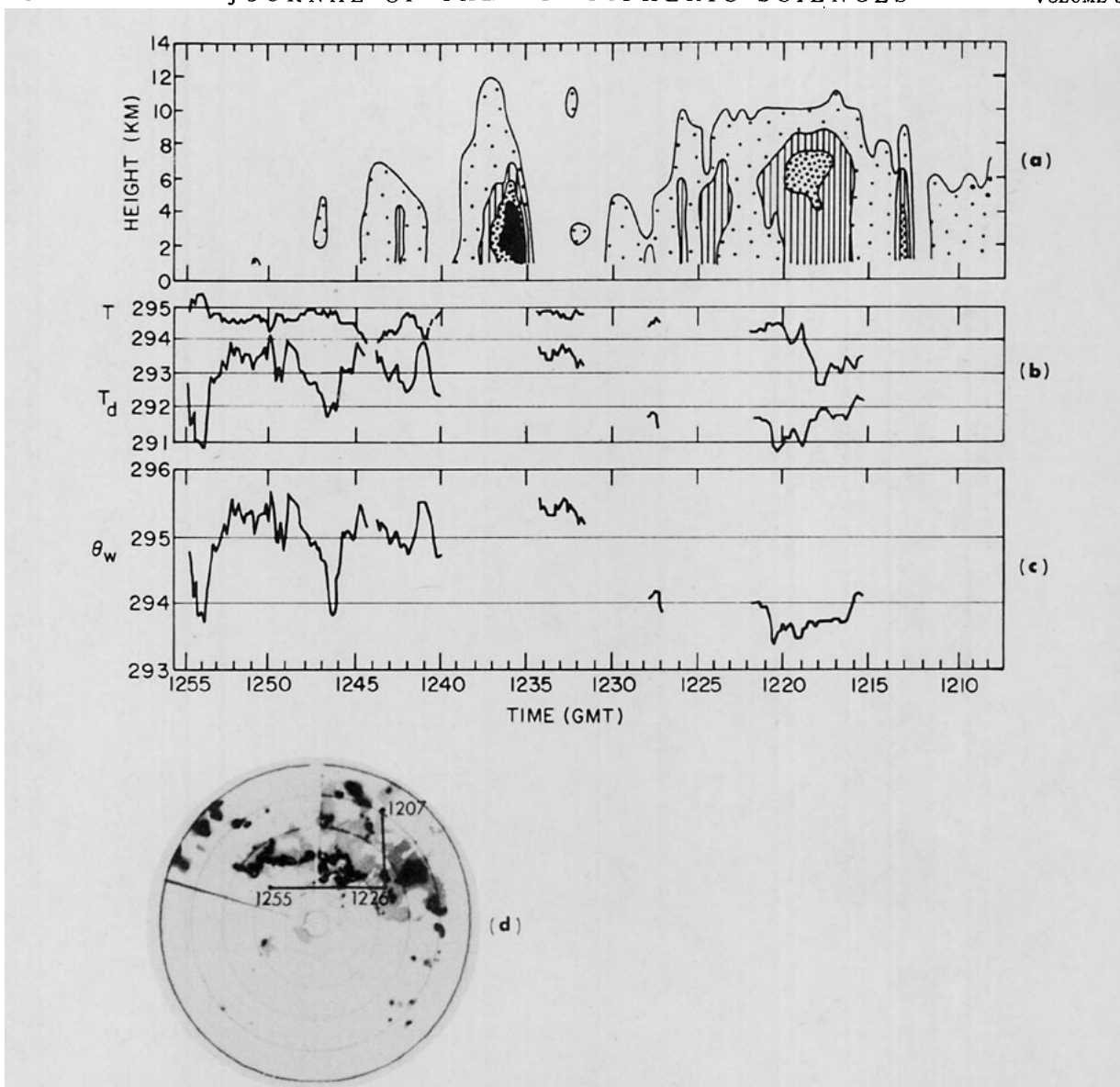

FIG. 8. (a) Vertical cross section of radar reflectivity derived from *Oceanographer* digital radar data for 1215–1300 GMT 5 September 1974, along the flight path of the National Center for Atmospheric Research's (NCAR) *Electra* aircraft. Outside contour is boundary of weakest detectable echo, and inside contours are for 28, 33 and 38 dBZ. (b) Ten-second averages of temperature T and dew point T_d measured on board the *Electra* at the flight level of 450 m. Gaps in the traces of T and T_d indicate unreliable data. (c) Wet-bulb potential temperature at flight level calculated from 10 s averages of T and T_d. (d) Horizontal display of the *Oceanographer* radar 1230 GMT 5 September 1974 showing the flight path of the aircraft. Shading thresholds same as Fig. 6.

scale downdraft in the area of horizontally uniform precipitation to explain the low values of θ_w observed there. The comparative dryness of the low-θ_w air argues for evaporational cooling being an important mechanism in the initiation and maintenance of the mesoscale downdraft, as suggested by Zipser (1969) and demonstrated numerically by Brown (1979).

Aircraft wind observations at the 450 m level showed evidence of convective-scale (as opposed to mesoscale) downdraft activity at the leading edge of E1 when the aircraft passed through an intense convective cell between 1235 and 1240 (Fig. 9). The southwesterly winds between 1231 and 1234, and between 1238 and 1242 were consistent with the larger scale low-level winds shown in Fig. 2c. Between 1235 and 1237, however, the low-level flow toward the mesoscale feature was perturbed in a manner consistent with the presence of strong outflow in the area of heavy precipitation. Such outflow suggests the presence of a downdraft. The small horizontal scale of the wind perturbation and its association with the heavy rainfall beneath a convective core both point to the downdraft as having been of convective scale.

The vertical cross sections shown in Fig. 7 all con-

tain an additional feature not included in the prototype shown in Fig. 1—shallow echoes ahead of and isolated from the mesoscale precipitation feature. While some such echoes dissipated before the mesoscale feature overtook them, others became incorporated into the leading edge and influenced the development of intense convection there. As this process occurred, the leading edge of the precipitation feature became irregular in shape (Figs. 6b–6d). Where the leading edge was concave outward, low-level outflow from convective-scale downdrafts led to the development of convection in the gaps between intense echo elements in a manner similar to that illustrated in Fig. 2. Both low-level convergence and moisture supply were enhanced due to the presence of the smaller echoes. Fig. 10 shows two examples of E1's interaction with smaller echoes along an irregular leading edge. In each case, intense cores of heavy rainfall at the later time (areas shaded by slanted lines) occurred preferentially in locations that were at the earlier time partially surrounded by irregularities in the leading edge of the mesoscale feature and isolated echoes in advance of the leading edge (echoes at the earlier time are shown by light shading and dots). The southeastern portion of the leading edge, which was preceded by fewer isolated echoes, developed in both cases fewer new intense cores and propagated southwestward less rapidly than the portion preceded by the larger isolated echoes.

b. Feature W1

Feature W1 provided a particularly good example of a mesoscale precipitation feature in its formative stage as a group of isolated small echoes. At 0000 (Fig. 3a) these echoes were aligned roughly parallel to the west-northwesterly surface wind in their vicinity (Leary, 1979, Fig. 2a). Their southeasterly motion between 0000 and 0600 (Fig. 4a) brought them into a region of southwesterly surface winds (Leary, 1979, Fig. 2b). There, the echoes were oriented nearly perpendicular to the southwesterly winds, and further development due to enhanced low-level convergence was rapid.

Fig. 11 shows horizontal and vertical cross sections through W1 during three different stages of its life

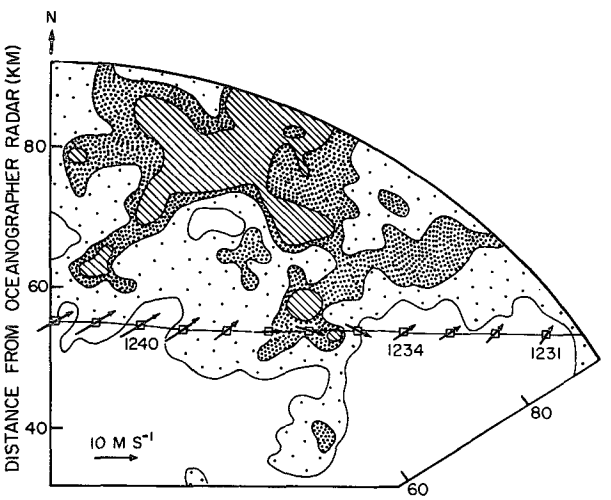

FIG. 9. Ten-second average winds at 1 min intervals along the flight path of the National Center for Atmospheric Research's (NCAR) *Electra* aircraft from 1231–1242 GMT 5 September 1974 and the radar reflectivity pattern observed by the *Oceanographer* radar at 1230 GMT. Outside contour of radar echo is boundary of weakest detectable echo, and inside contours are for 38 dBZ or 14 mm h^{-1} and 43 dBZ or 36 mm h^{-1}.

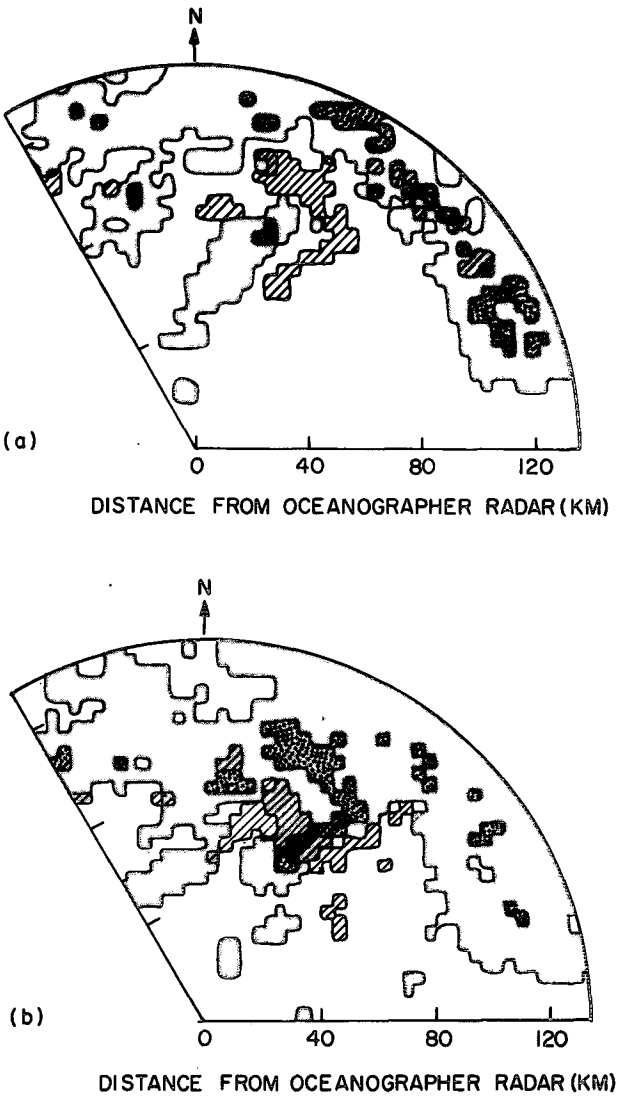

FIG. 10. (a) Echo cores at 1200 (areas outlined by slanted lines) of intensity 38 dBZ or 14 mm h^{-1} or greater superimposed on the radar echo pattern for 1045 GMT. The outer contour of the 1045 echo pattern is for the minimum detectable signal and the inner contour (enclosing the area shaded with large dots) is for 38 dBZ or 14 mm h^{-1}. (b) Echo cores at 1300, superimposed on the radar echo pattern for 1200. Contours same as for (a). Times are GMT on 5 September 1974.

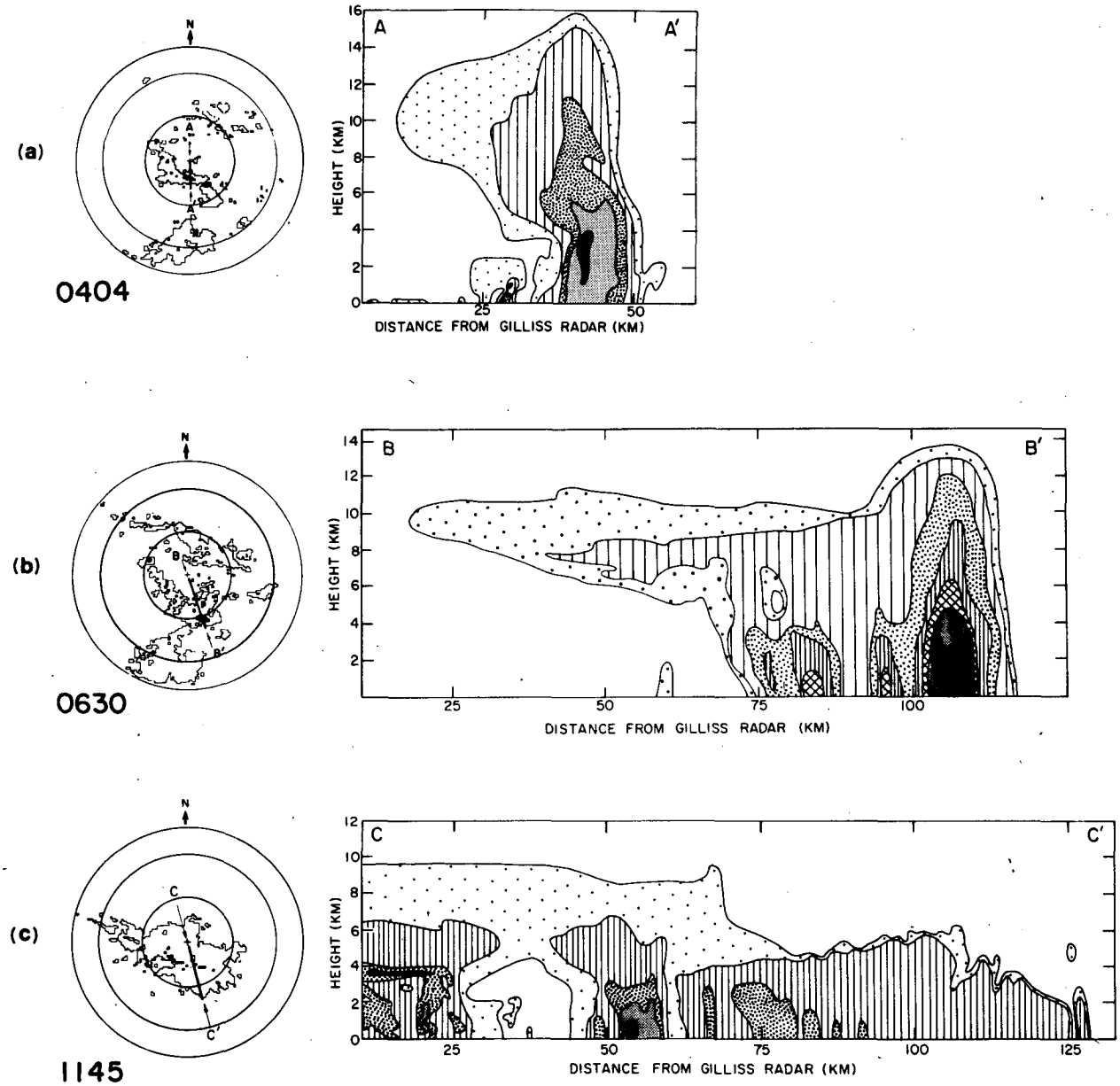

FIG. 11. Mesoscale precipitation feature W1 as viewed by the *Gilliss* radar in horizontal and vertical cross sections during its life cycle. On horizontal cross sections the outside contour is for 11 dBZ or 0.1 mm h^{-1}, the inner contour is for 41 dBZ or 25 mm h^{-1}, range marks are at 100, 200 and 256 km, and labeled lines identify the vertical cross sections. On the vertical cross sections the outside contour is for the weakest detectable echo and the inner contours are for (a) 21, 31, 41 and 51 dBZ; (b) 21, 26, 31, 36, 41 and 46 dBZ; (c) 21, 31, 36 and 41 dBZ. Times are GMT on 5 September 1974.

cycle. By 0404 (Fig. 11a) feature W1 possessed characteristics of both a formative and an intensifying mesoscale precipitation feature. It resembled a formative mesoscale feature (Fig. 1a) in that the most intense portions of the band, of which the vertical cross section in Fig. 11a was an example, exhibited only a single precipitation maximum along a line oriented across the band. In other respects, however, the feature was clearly intensifying (Fig. 1b). Its vertical development and high precipitation rates were particularly impressive. Along the direction of the band, the individual echoes had merged, giving the horizontal cross section of W1 in Fig. 11a the appearance of an intensifying precipitation feature. An overhang of precipitation particles at high levels in the vertical cross section at 0404 was another indicator of intensification.

By 0630 (Fig. 11b) W1 had broadened. The heaviest precipitation lay along the leading edge, with older cells situated to the rear. The overhang at the 10 km level extended more than 50 km beyond the surface

precipitation pattern. Feature W1 never developed the deep layer of horizontally uniform precipitation accompanied by a well-defined radar bright band that characterizes a mature mesoscale precipitation feature (Figs. 1c–1d). Between 0600 and 1200 its convective cells gradually grew less intense and more shallow.

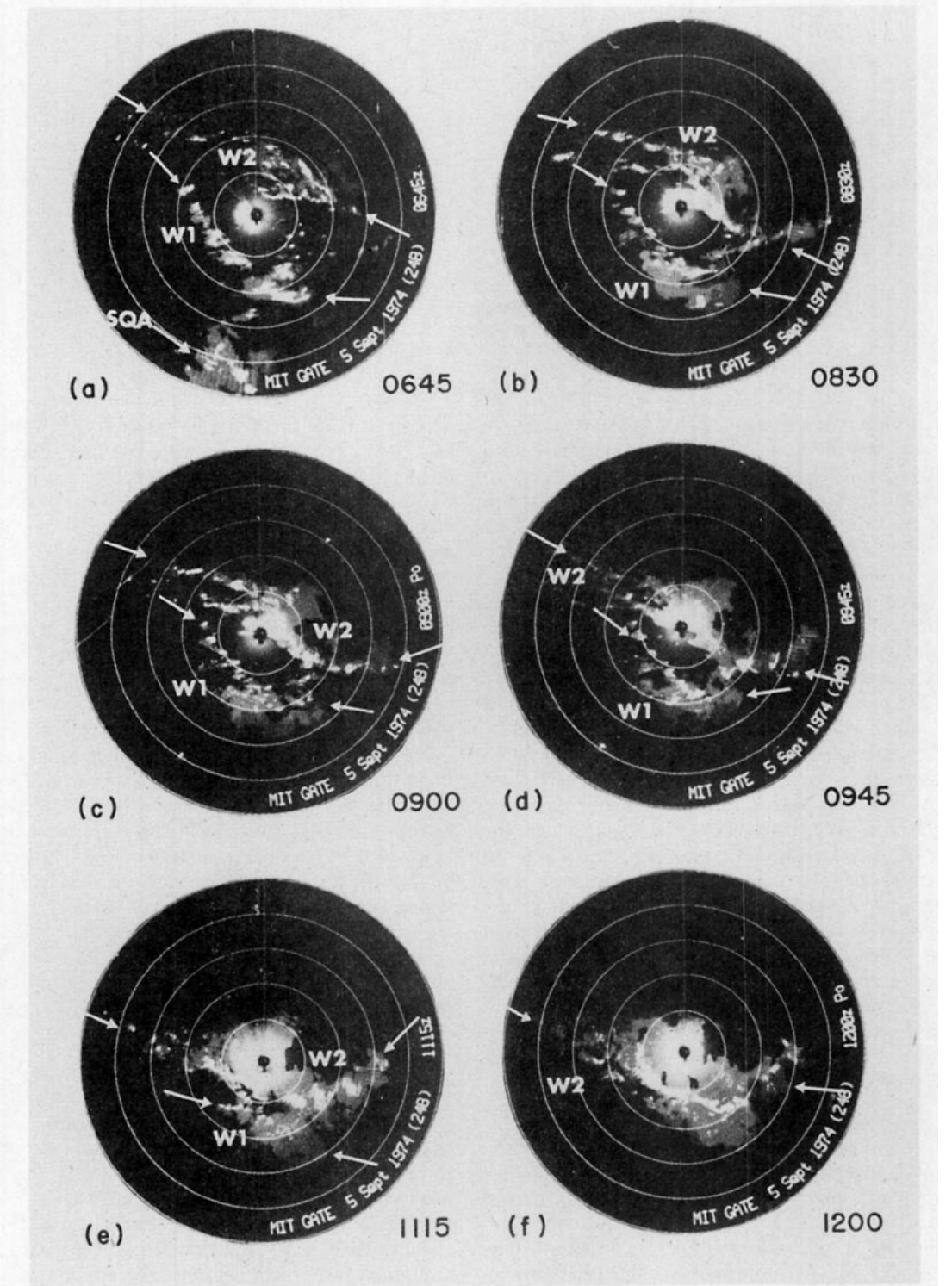

FIG. 12. Sequence of horizontal cross sections from the *Gilliss* radar showing mesoscale precipitation feature W2 overtaking feature W1. Shading thresholds are for 11 dBZ or 0.1 mm h^{-1} (gray) and 36 dBZ or 10 mm h^{-1} (white). Range marks are at 50, 100, 150, 200 and 250 km. Times are GMT.

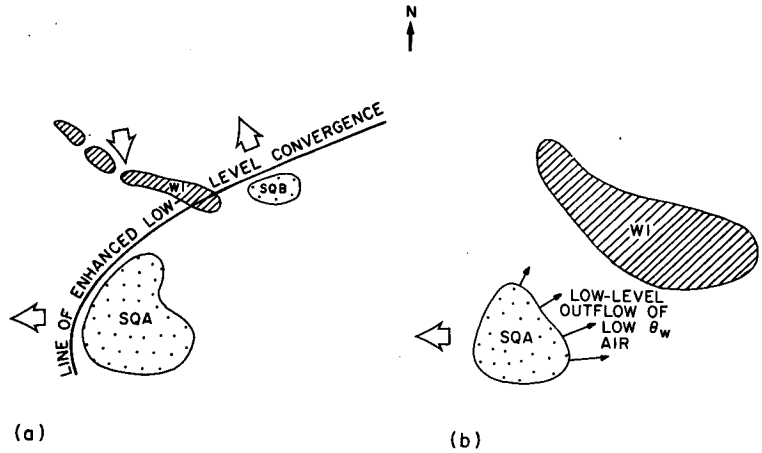

FIG. 13. Schematic showing the interaction of the squall-line system (SQA and SQB) with mesoscale precipitation feature W1 (a) when the squall-line system enhanced convection in W1 and (b) when the squall-line system inhibited development of W1.

During this interval it ceased to propagate and (as shown in Fig. 12) was overtaken by and incorporated into feature W2. At 1145 (Fig. 11c) a vertical cross section showed a rather sharp boundary at a range of 60 km between the cellular pattern of the leading edge of W2 and the shallower and lighter precipitation associated with the dissipating feature W1.

Both enhanced development of W1 and its early dissipation can be attributed to its interactions with the squall-line system (SQ). Fig. 13 illustrates the two processes schematically (cf. Fig. 12a). We postulate that as SQ moved westward (Fig. 13a) an arc-shaped line of enhanced low-level convergence was present along the leading edge of cool downdraft air deposited by the formerly more active squall-line system (Houze, 1977). As this line passed through the southeastward moving feature W1, convection was enhanced in the younger feature. This would explain why the precipitation pattern at 0600 in W1 (Figs. 3b, 11a) was most intense at its intersection with the leading edge of the squall-line system. Later, when the line of enhanced low-level convergence was no longer a distinct feature, a different situation prevailed behind the feature SQA (Fig. 13b). There, the cool, dry, low-θ_w mesoscale downdraft air from SQA apparently suppressed convection and hindered further development and propagation of the precipitation feature W1.

c. *Feature N*

Like W2, feature N had a distinct formative stage as a group of isolated, shallow echoes. As it moved southward into the radar network between 0000 and 0600 (Fig. 4a) its great length became apparent. The line of echoes which comprised N coincided with an even longer narrow cloud line associated with cyclonic shear in the low-level wind field (Leary, 1979, Fig. 3). This line of clouds was a persistent and striking feature in satellite photographs between 4 and 7 September. It was most clearly defined in visible satellite imagery where it was seen to consist primarily of shallow clouds. However, this cloud line could not be completely distinguished in satellite pictures when a portion of it moved into the region shielded by cirrus from the deep convective clouds in the area covered by the GATE radars on 5 September. Extrapolation of the satellite positions of N into the region covered by cirrus, however, matches the position, orientation and motion of the feature N observed on radar, making it clear that this precipitation feature was an extension of the eastern portion of the cloud line observed by satellite.

Fig. 14 shows two vertical and horizontal cross sections through feature N during its formative stage. In both the western portion of N (Fig. 14a), north of feature W1 (Fig. 3b), and in the eastern portion of N (Fig. 14b), to the north of feature E1, the echoes exhibited the same structure—convective cells possessing strong horizontal gradients of radar reflectivity organized into a band much longer than it was wide.

The intensification of feature N did not proceed uniformly along its great length. Instead, it evolved into two major mesoscale features, E2 and W2, as well as several minor features.

d. *Feature W2*

At 0601 (Fig. 15a), the western portion of N was oriented from northwest to southeast. It was still embedded in a northwesterly flow at the surface and lay just north of the convergence line where the northwesterlies were met by southwesterlies to the south (Leary, 1978, Fig. 2b). Continued southward motion brought N into a southwesterly surface flow, where low-level convergence was enhanced because the feature was then oriented perpendicular to the surface winds and moving in a direction opposite to the surface flow.

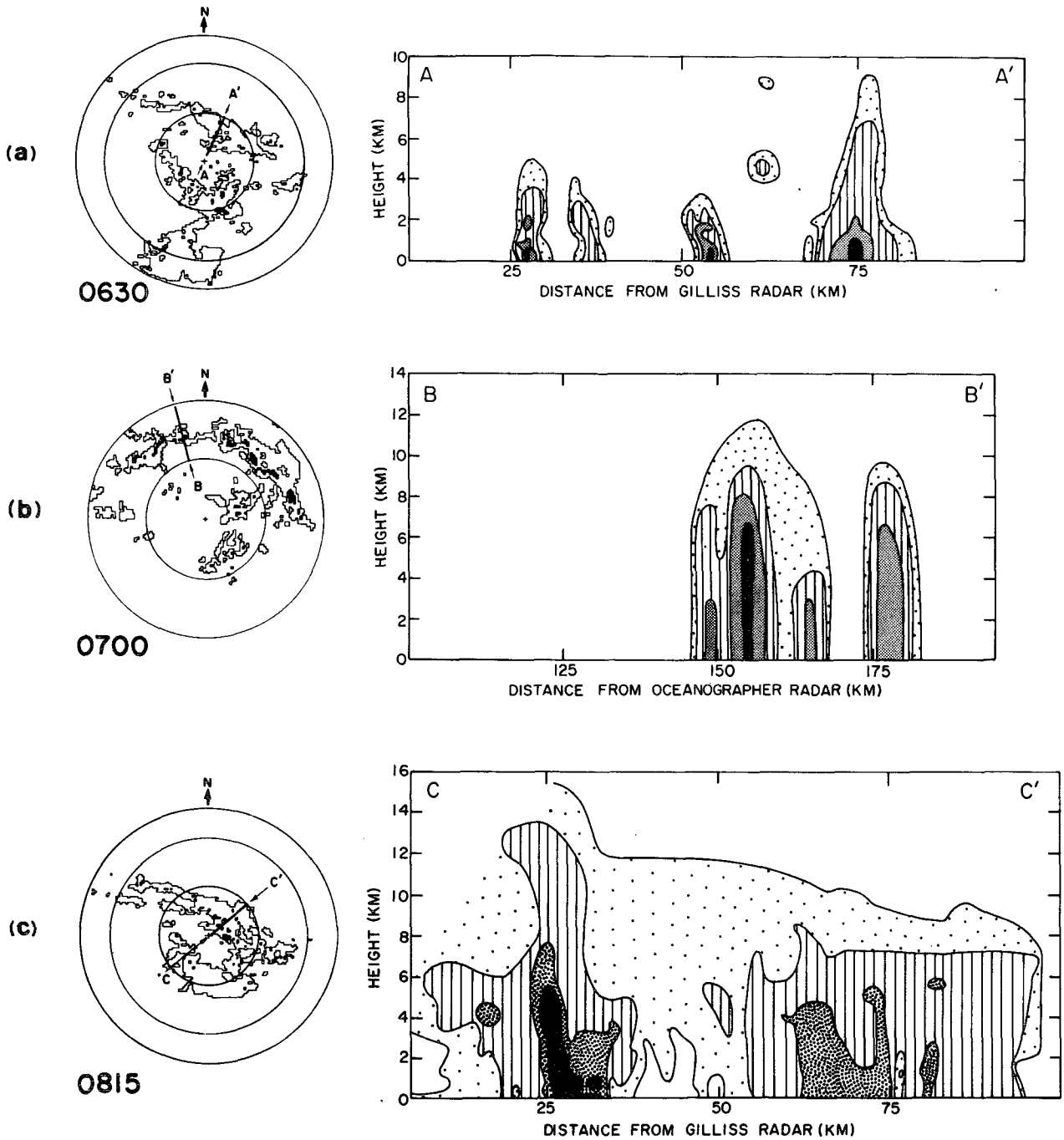

FIG. 14. Mesoscale precipitation feature N as viewed by the *Gilliss* [(a) and (c)] and *Oceanographer* (b) radars in horizontal and vertical cross sections during its life cycle. (a) and (c) On horizontal cross sections the outer contour is for 11 dBZ or 0.1 mm h^{-1}, the inner contour is for 41 dBZ or 25 mm h^{-1}, range marks are at 100, 200 and 256 km, and labeled lines identify the vertical cross sections. On the vertical cross sections,the outside contour is for the weakest detectable echo and the inner contours are for (a) 21, 31 and 36 dBZ; (c) 21, 31 and 41 dBZ. (b) On horizontal cross sections the outer contour is for the weakest detectable echo, the inner contour is for 38 dBZ or 14 mm h^{-1}, range marks are for 110 and 220 km, and labeled line identifies the vertical cross section. On the vertical cross section, the outside contour is for the weakest detectable echo, and the inner contours are for 28, 33 and 38 dBZ. Times are GMT on 5 September 1974.

Along with this enhanced convergence came intensification in the form of feature W2.

As early as 0601 (Fig. 15a) there was new echo development on and just ahead of the leading edge of the western portion of N that became feature W2. The vertical cross section at 0630 in Fig. 14a cuts through

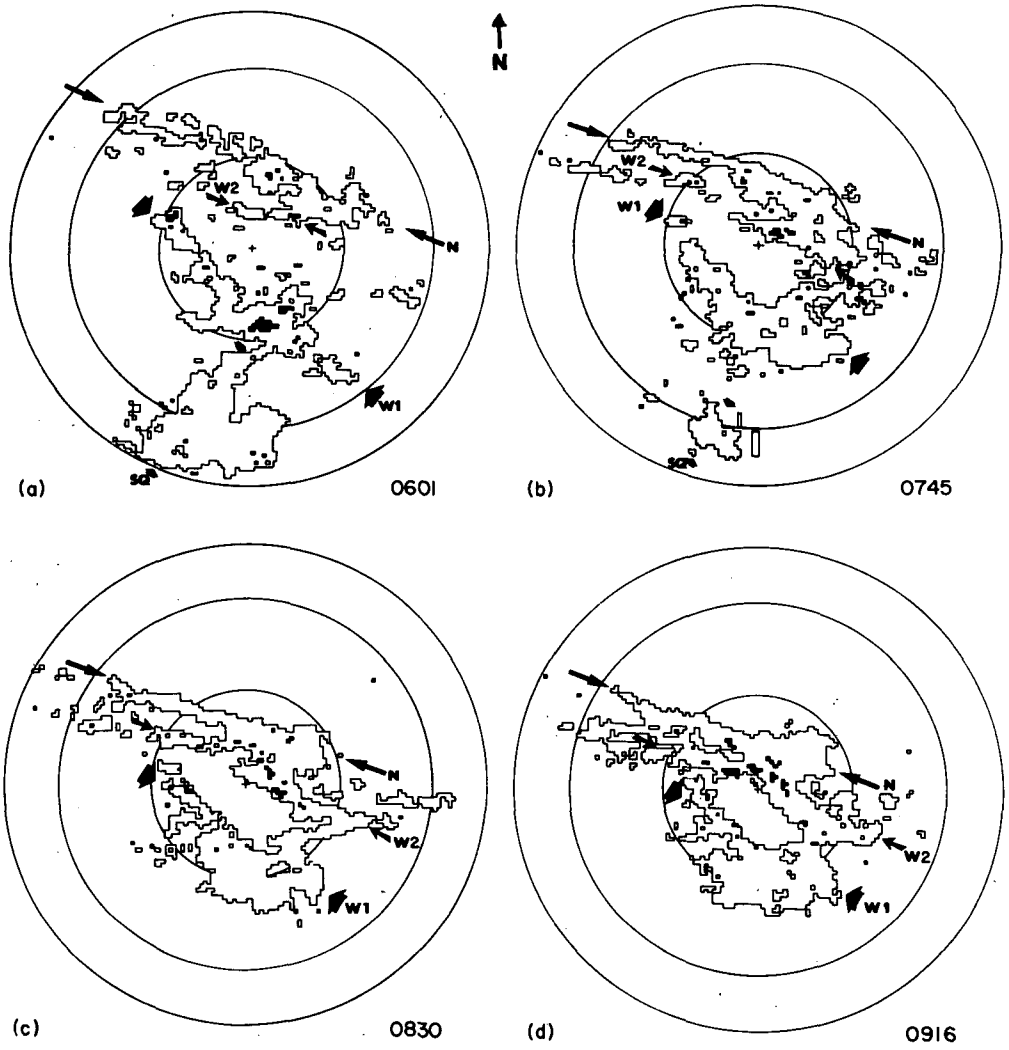

FIG. 15. Sequence of horizontal cross sections from the *Gilliss* radar showing the development of mesoscale precipitation feature W2 on 5 September 1974. The outside contour is for 11 dBZ or 0.1 mm h^{-1} and the inner contour is for 41 dBZ or 25 mm h^{-1}. Range marks are 100, 200 and 256 km. Times are GMT.

two of the newly formed echoes at ranges between 25 and 40 km, revealing them to be quite shallow but possessing the strong horizontal gradients and high maximum values of reflectivity characteristic of convective cells. During the time period 0601–0916 (Figs. 15a–15d), further development took place along the line W2 ahead of N until, by 0916 (Fig. 15d), most of the intense convective cells lay along W2, and N was comprised mainly of dissipating cells. This development of W2 resembles SQ, the squall-line system, which propagated by the systematic formation of discrete squall-line elements ahead of its leading edge while older convective elements dissipated to the rear of the leading edge and blended into a trailing region of horizontally uniform rain (Houze, 1977). Fig. 14c shows a vertical cross section through W2 and N, illustrating the intense convection associated with the new line W2 at ranges between 15 and 40 km, as well as the less intense and more horizontally uniform precipitation associated with the dissipating portions of N at ranges between 50 and 100 km. In contrast to Fig. 14c, Fig. 16a shows a vertical cross section of a portion of W2 that was well ahead of N. It contained well-developed convective cells with the strong horizontal reflectivity gradient and the upper level overhang of precipitation particles characteristic of an intensifying mesoscale precipitation feature (Fig. 1b).

By 1145 (Fig. 16b), W2 possessed all the characteristics of a mature mesoscale precipitation feature (Fig. 1c). These included intense precipitation and extensive vertical development in convective cells (sections B1–B1′ in Fig. 16b), a well-defined radar bright band at the melting level in a large area of horizontally uniform precipitation, and an overhang of precipitation

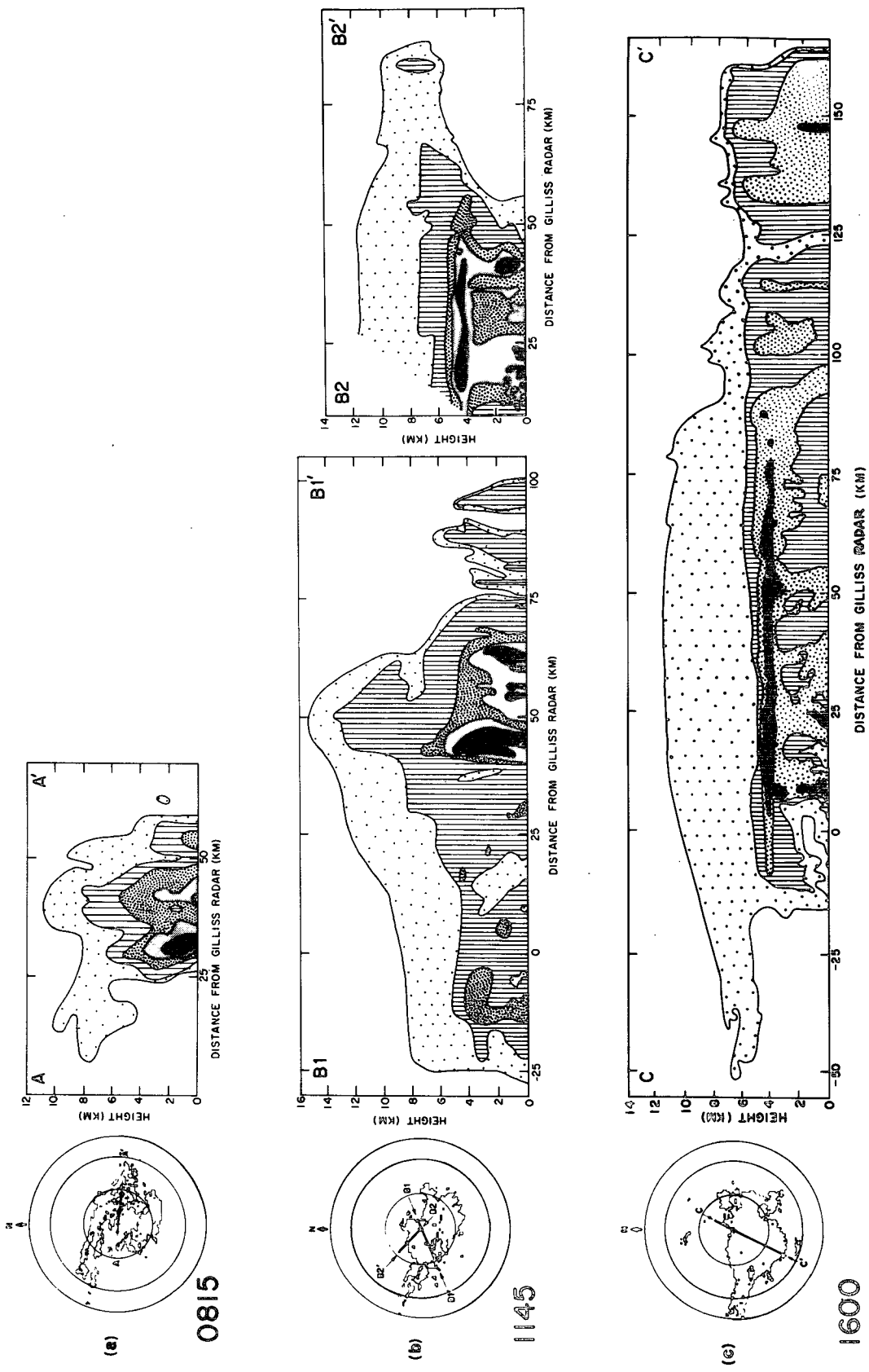

FIG. 16. Mesoscale precipitation feature W2 as viewed by the *Gilliss* radar in horizontal and vertical cross sections during its life cycle. On horizontal cross sections the outside contour is for 11 dBZ or 0.1 mm h^{-1}, the inner contour is for 41 dBZ or 25 mm h^{-1}, range marks are at 100, 200 and 256 km, and labeled lines identify the vertical cross sections. On the vertical cross sections, the outside contour is for the weakest detectable echo and the inner contours are for (a) 21, 31, 41 and 46 dBZ; (b) Section B1–B1′: 21, 31, 36 and 41 dBZ; Section B2–B2′: 21, 26, 31 and 36 dBZ; (c) 26, 31 and 36 dBZ. Times are GMT on 5 September 1974.

particles downwind at upper levels (sections B2–B2′ in Fig. 16b). Some of the most intense convective cells were to the rear of the edge of the echo in Fig. 16b on account of the presence of the remnants of feature W1 ahead of the leading edge of W2 (cf. Fig. 12).

At 1600 (Fig. 16c) feature W2 was in the dissipating stage of its life cycle (Fig. 1d). Echo tops had been decreasing in height from 1145 and the convective cells near the leading edge at ranges >100 km had decreased in both height and intensity. A large region of horizontally uniform precipitation was present, along with an extensive, well-defined bright band at the melting level. To the rear of W2 an overhang of precipitation spread northeast of the radar, suggesting evaporation in unsaturated sinking air. Fig. 16c bears a strong resemblance to the vertical structure of SQ (Houze, 1977, Figs. 2 and 25), in which the presence of a mesoscale unsaturated downdraft in the region of horizontally uniform precipitation was inferred from thermodynamic data. The dissipating stage of W2

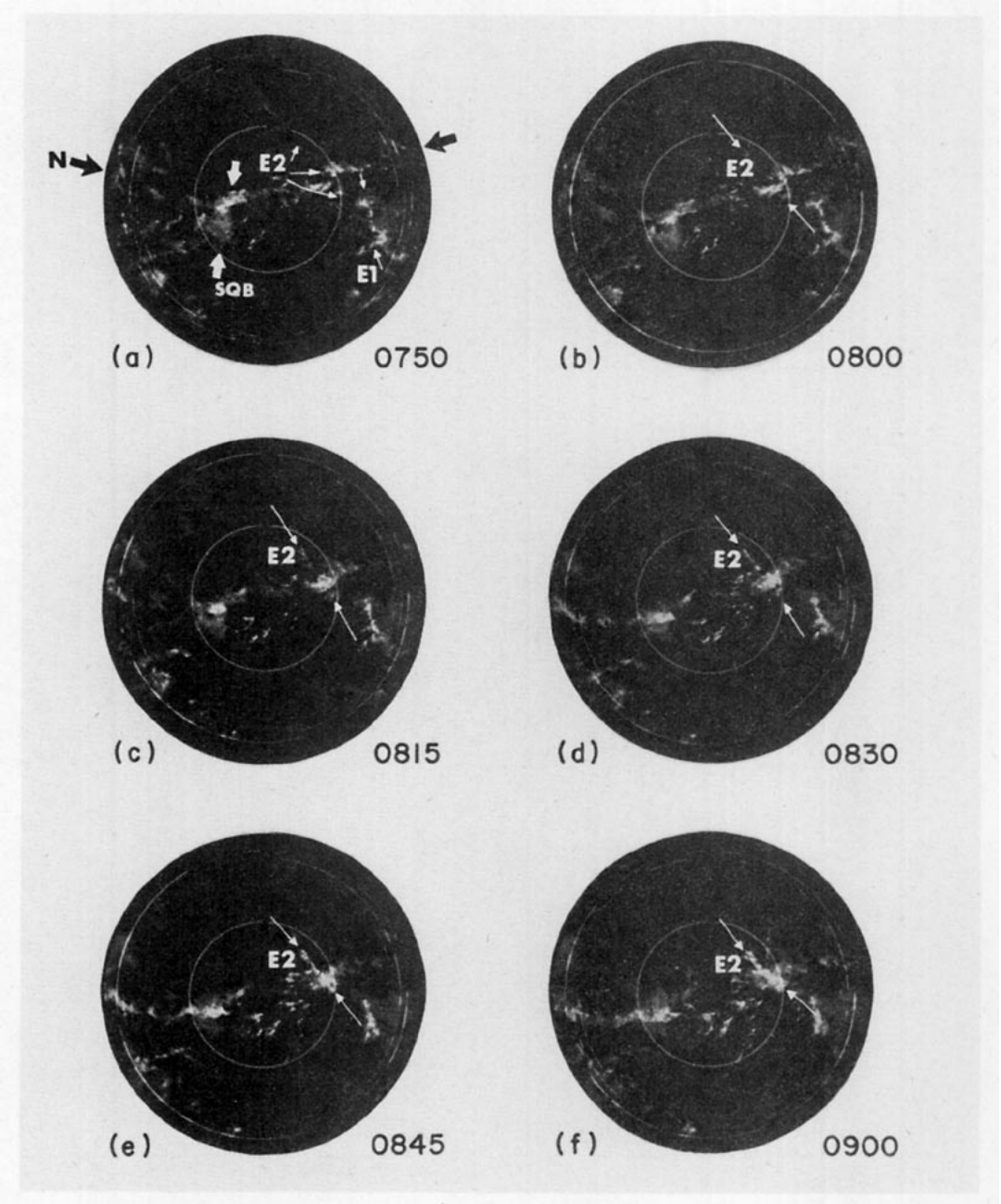

FIG. 17. Sequence of horizontal cross sections from the *Quadra* radar showing the development of mesoscale precipitation feature E2 on 5 September 1974. Shading thresholds are for 12 dBZ or 0.1 mm h^{-1} (dark gray), 22 dBZ or 0.6 mm h^{-1} (light gray), and 32 dBZ or 3.6 mm h^{-1} (white). Range marks are at 100 and 200 km. Times are GMT.

continued to at least 0000 on 6 September (Fig. 3h), when the feature passed out of radar range. This longevity could well be due to persistent low-level southwesterly inflow to the leading edge of W2 which continued to be a feature of the surface wind field through 0000 on 6 September (Leary, 1979, Fig. 2e).

e. Feature E2

By 0800 (Fig. 3c) the portion of feature N to the east of 23°W had a northeast-to-southwest orientation, roughly parallel to the 0600 surface winds and coincident with the line of confluence they define (Leary, 1979, Fig. 2b). Intensification of the eastern portion of N took the course illustrated by the photographs of the *Quadra* radar scope shown in Fig. 17. At 0750 (Fig. 17a), feature E2 consisted only of three small groups of echoes. During the next hour more echoes formed along a line oriented from northwest to southeast, connecting the three original groups of echoes (Fig. 17b–17e). Simultaneously, the portion of feature N that intersected this line grew in both size and intensity. This intensification gave feature E2 the characteristic size and cohesive appearance of a mesoscale precipitation feature by 0900 (Fig. 17f). That E2 formed with the same orientation as E1 and in such close association with N (Fig. 17a) was reminiscent of the role the remains of the squall-line system played in the formation of W1 (Fig. 13a). The enhanced convergence associated with the northwest to southeast orientation of E1 was analogous to the low-level convergence associated with SQ, and the small, isolated echoes (Fig. 17a) that later became feature E2 were analogous to the line of isolated echoes from which feature W1 formed.

The portion of feature N to the west of E2 (Fig. 17) continued to produce precipitation for several hours, and during that time influenced the interaction of features E1 and E2. At 0929 (Fig. 18a) the precipitation associated with E1, E2 and the remnants of N formed three rather distinct areas, as defined by the position and orientation of their intense echo cores, and the minimum of radar reflectivity at their boundaries. By 1059 (Fig. 18b), however, the advance of E1 and E2 toward N had resulted in a unification of the rain areas into a single mass of echo. Just as the outflow from isolated echoes contributed to the development and propagation of E1 (Fig. 10), we infer that outflow from the remnants of feature N (Fig. 18a) interacted with outflow from E1 and E2 to produce new convection which filled in the gaps in the echo pattern between N, E1 and E2. This merger of rain areas gave the eastern half of the double cloud cluster its distinctive shape at 1200 (Fig. 3d; Leary, 1979, Figs. 1, 2c). We propose that outflow from nearby rain areas produces an enhanced low-level convergence in the intervening echo-free region. This enhanced low-level convergence then leads to the production of echoes in the region that was originally echo-free, thus resulting in

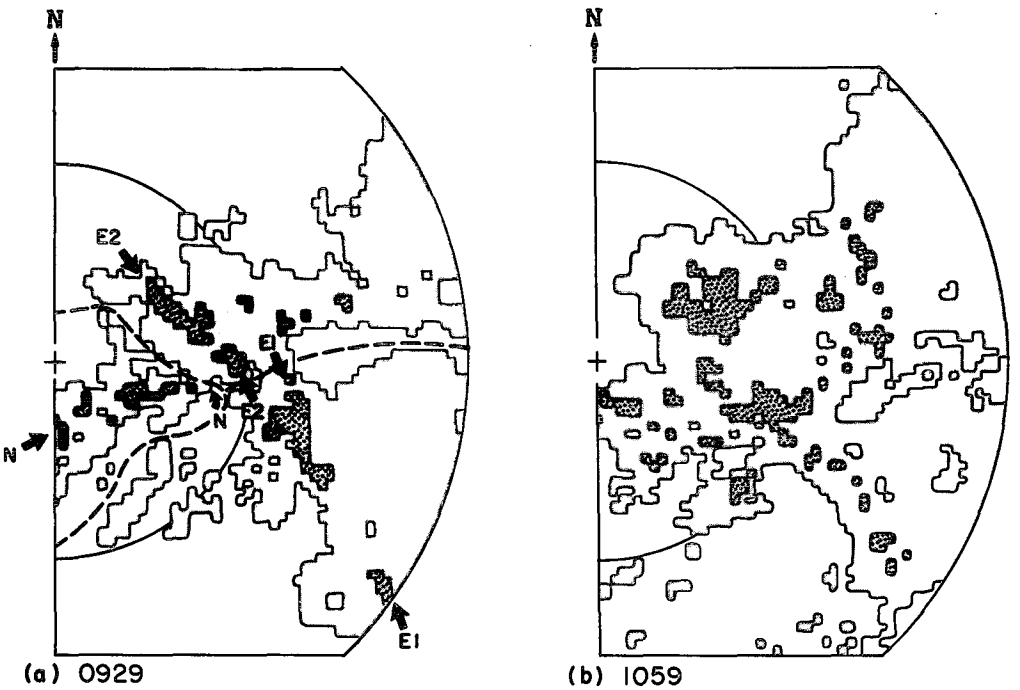

FIG. 18. Horizontal cross sections from *Quadra* radar data showing the merger of portions of mesoscale precipitation features N, E1 and E2. Dashed lines in (a) denote the boundaries between the mesoscale features. The outer contour is for the weakest detectable echo and the inner contour is for 34 dBZ or 7 mm h^{-1}. Times are GMT.

the echo mergers which Lopez (1976) and Houze and Cheng (1977) have found to be a common feature of precipitation areas of all sizes in the tropics.

Lack of availability of the *Quadra* digital radar data for the full conical scan sequence limited our elucidation of the three-dimensional structure and life cycle of feature E1 to those portions of it that lay within range of the *Oceanographer* radar, or that could be determined by the study of horizontal cross sections only. The vertical cross sections which intersected E2 did so at such great distances from the *Oceanographer* radar ($\gtrsim$150 km) that poor vertical resolution severely limited the detail they could provide, but in no way did they contradict the general pattern of the evolution of mesoscale precipitation features presented in Section 3 and described in the previous subsections. After its intensification from a group of isolated echoes and the eastern portion of feature N, the development of E2, as viewed in horizontal cross sections, closely paralleled that of feature E1 with which it interacted. The parallel development can be seen in Figs. 3d–3g. We infer from these similarities and the lack of contradiction from the available three-dimensional radar data that similar dynamic and thermodynamic processes were present in features E1 and E2.

The easternmost portions of feature N were located beyond the range of the GATE radars. Satellite data suggest the presence of some intense convection to the east of feature E2 which also contributed to the eastern half of the double cloud cluster.

6. Conclusions

Virtually all of the precipitation in the tropical cloud cluster of 5 September 1974 was associated with six mesoscale precipitation features whose lifetimes varied between 8 and 24 h, and whose maximum horizontal dimensions ranged from 190–580 km. One of these was the tropical squall-line system whose structure and dynamics have been described by Houze (1977). The mesoscale precipitation features were sufficiently similar to one another to permit us to extend Houze's (1977) model for the structure of the squall-line system and construct a prototype (Fig. 1) for the structure and life cycle of a mesoscale precipitation feature. This prototype is general enough to describe both the squall-line system and the non-squall precipitation features in the cloud cluster of 5 September. The complexity of the observed precipitation pattern (Fig. 3) was a result of interactions among the mesoscale precipitation features and between these features and isolated smaller echoes.

A mesoscale precipitation feature develops from several isolated convective cells aligned perpendicular to the low-level winds in a region of convergence. The alignment of the cells perpendicular to the low-level wind appears to be crucial to the intensification of the precipitation feature because this orientation favors the development of new convective cells between and upwind of the existing cells, where outflow from convective-scale downdrafts enhances low-level convergence. In this way, the leading edge of the line of precipitating cumulonimbus clouds propagates upwind with respect to the surface flow, no matter what the direction of the upper level winds. Convergence at low levels along the leading edge provides a steady supply of moist inflow air to buoyant cumulonimbus updrafts which extend to the upper troposphere. These updrafts are the "hot towers" that Riehl and Malkus (1958) deduced must exist to accomplish the vertical transports of mass and heat required of the general circulation in the tropics. The mesoscale precipitation areas which we have described are the entities within which these "hot towers" occur.

Besides "hot towers," the mesoscale precipitation features in cloud clusters exhibit other characteristic and dynamically important features. As an intensifying mesoscale precipitation feature propagates, new convective cells develop along its leading edge faster than the older cells to the rear can dissipate. This process broadens the precipitation feature along its direction of motion, and leads to the development of a large ($\sim 10^4$ km^2) area of lighter, horizontally uniform precipitation to the rear of the vigorous convective-scale updrafts and downdrafts along the leading edge. Its large size implies that vertical velocities and precipitation rates of rather small magnitude in this region can make a substantial contribution to the mass, heat, moisture, and momentum budgets of the mesoscale precipitation features which make up the cloud cluster.

The longevity ($\gtrsim$10 h) of this area and the large total amount of precipitation it contains suggest that its existence may be due to more than a blending together of dissipating convective cells. Brown's (1979) dynamical model of a tropical disturbance developed an extensive area of mesoscale uplift in a nimbostratus anvil cloud which could help account for the large amounts of precipitation observed in the rear of the active convective cells. The region of horizontally uniform precipitation shows evidence of possessing a mesoscale downdraft. Aircraft observations in this region at 450 m confirm that air at this level is subsiding, and the horizontally stratified radar reflectivity pattern strongly suggests that the subsidence is mesoscale in extent and not interrupted by embedded convection. In Brown's (1979) model, cooling due to the evaporation of falling rain initiated and maintained the mesoscale downdraft. The radar bright band at the melting level in this region of the mature and dissipating mesoscale precipitation feature is evidence of further cooling there.

Our generalization of the structure and behavior of a mesoscale precipitation feature to include both squall and non-squall cases makes it possible to formulate models general enough to calculate vertical fluxes of mass, heat and momentum for an arbitrary cloud cluster or an entire population of cloud clusters.

Acknowledgments. The following GATE scientists provided the authors with data: Dr. Geoffrey L. Austin, Dr. Pauline M. Austin, Mr. Spiros G. Geotis, Dr. Michael D. Hudlow, Mr. Frank D. Marks, Dr. David W. Martin, Mr. Ernest E. Recker, Prof. Richard J. Reed, Dr. David Suchman and Dr. Edward J. Zipser.

Dr. Edward J. Zipser arranged for the authors to visit with his GATE Group at the National Center for Atmospheric Research during the course of this study. We thank Prof. Richard J. Reed for reading the manuscript. The figures were drafted by Mrs. Kay Moore.

This research was supported by the Global Atmospheric Research Program, National Science Foundation, and the U.S. GATE Project Office, National Oceanic and Atmospheric Administration, Grant ATM74-14830.

REFERENCES

Betts, A. K., R. W. Grover and M. W. Moncrieff, 1976: Structure and motion of tropical squall-lines over Venezuela. *Quart. J. Roy. Meteor. Soc.*, **102**, 395–404.

Brown, J. M., 1979: Mesoscale unsaturated downdrafts driven by rainfall evaporation: A numerical study. *J. Atmos. Sci.*, **36** (in press).

EDS, 1975: *GATE Data Catalog.* [Available from GATE World Data Center A, National Climatic Center, Environmental Data Service (EDS), NOAA, Federal Building, Asheville, North Carolina.]

Frank, N. L., 1970: Atlantic tropical systems of 1969. *Mon. Wea. Rev.*, **98**, 307–314.

GARP Report, 1970: *The Planning of GARP Tropical Experiments.* Global Atmospheric Research Programme (GARP), Publ. Ser. No. 4, WMO, Geneva, 78 pp.

Gray, W. M., 1968: Global view of the origin of tropical disturbances and storms. *Mon. Wea. Rev.*, **96**, 669–700.

Houze, R. A., Jr., 1977: Structure and dynamics of a tropical squall-line system. *Mon. Wea. Rev.*, **105**, 1540–1567.

——, and C.-P. Cheng, 1977: Radar characteristics of tropical convection observed during GATE: Mean properties and trends over the summer season. *Mon. Wea. Rev.*, **105**, 964–980.

Johnson, R. H., 1976: The role of convective-scale precipitation downdrafts in cumulus and synoptic-scale interactions. *J. Atmos. Sci.*, **33**, 1890–1910.

Leary, C. A., 1979: Behavior of the wind field in the vicinity of a cloud cluster in the Intertropical Convergence Zone. *J. Atmos. Sci.*, **36** (in press).

——, and R. A. Houze, Jr., 1979: Melting and evaporation of hydrometeors in precipitation from the anvil clouds of deep tropical convection. *J. Atmos. Sci.*, **36** (in press).

Lopez, R. E., 1976: Radar characteristics of the cloud populations of tropical disturbances in the northwest Atlantic. *Mon. Wea. Rev.*, **104**, 268–283.

Martin, D. W., and O. Karst, 1969: A census of cloud systems over the tropical Pacific. Studies in Atmospheric Energetics Based on Aerospace Probings, Ann. Report, 1968, Space Science and Engineering Center, University of Wisconsin.

——, and V. E. Suomi, 1972: A satellite study of cloud clusters over the tropical North Atlantic Ocean. *Bull. Amer. Meteor. Soc.*, **53**, 135–156.

Ogura, Y., and H.-R. Cho, 1973: Diagnostic determination of cumulus cloud populations from observed large-scale variables. *J. Atmos. Sci.*, **30**, 1276–1286.

Payne, S. W., and M. M. McGarry, 1977: The relationship of satellite inferred convective activity to easterly waves over West Africa and the adjacent ocean during Phase III of GATE. *Mon. Wea. Rev.*, **105**, 413–420.

Riehl, H., and J. S. Malkus, 1958: On the heat balance in the equatorial trough zone. *Geophysica*, **6**, 503–538.

Yanai, M., S. Esbensen and J.-H. Chu, 1973: Determination of the bulk properties of tropical cloud clusters from large-scale heat and moisture budgets. *J. Atmos. Sci.*, **30**, 611–627.

Zipser, E. J., 1969: The role of organized unsaturated convective downdrafts in the structure and rapid decay of an equatorial disturbance. *J. Appl. Meteor.*, **8**, 799–814.

——, 1977: Mesoscale and convective-scale downdrafts as distinct components of squall-line structure. *Mon. Wea. Rev.*, **105**, 1568–1589.